Virology 482 (2015) 208–217

Contents lists available at ScienceDirect

Virology

journal homepage: www.elsevier.com/locate/yviro

Membrane association of a nonconserved viral protein confers virus ability to extend its host range

Sung-Hwan Kang, Aurélie Bak [1], Ok-Kyung Kim [2], Svetlana Y. Folimonova *

University of Florida, Plant Pathology Department, Gainesville, FL 32611, USA

ARTICLE INFO

Article history:
Received 26 February 2015
Returned to author for revisions
17 March 2015
Accepted 20 March 2015
Available online 14 April 2015

Keywords:
Citrus tristeza virus
Virus movement
Plant virus

ABSTRACT

Citrus tristeza virus (CTV), the largest and most complex member of the family *Closteroviridae*, encodes a unique protein, p33, which shows no homology with other known proteins, however, plays an important role in virus pathogenesis. In this study, we examined some of the characteristics of p33. We show that p33 is a membrane-associated protein that is inserted into the membrane via a transmembrane helix formed by hydrophobic amino acid residues at the C-terminal end of the protein. Removal of this transmembrane domain (TMD) dramatically altered the intracellular localization of p33. Moreover, the TMD alone was sufficient to confer membrane localization of an unrelated protein. Finally, a CTV variant that produced a truncated p33 lacking the TMD was unable to infect sour orange, one of the selected virus hosts, which infection requires p33, suggesting that membrane association of p33 is important for the ability of CTV to extend its host range.

Introduction

Citrus tristeza virus (CTV), the largest and most complex member of the family *Closteroviridae*, is a phloem-limited virus, which infects *Citrus* spp. and close relatives (Bar-Joseph et al., 1979; Dolja et al., 1994, 2006; Agranovsky, 1996; Karasev, 2000). CTV has significantly impacted citrus industries in many different countries all over the world by causing two types of disease—quick decline and stem pitting, which led to dramatic losses of fruit yield and death of millions of trees (reviewed in Moreno et al., 2008). CTV has a 19.3 kb positive-sense RNA genome organized into 12 open reading frames (ORFs; Fig. 1), which encode proteins that function at different stages of the virus life cycle (Pappu et al., 1994; Karasev et al., 1995; Karasev, 2000). ORFs 1a and 1b are expressed from the genomic RNA and encode polyproteins involved in virus replication. The other ten genes in the 3′ half of the genome are expressed by 3′ co-terminal subgenomic RNAs (sgRNA; Hilf et al., 1995; Karasev et al., 1997). Five of these genes represent a signature gene block conserved among the members of the *Closteroviridae* and encode a hydrophobic protein p6, p65 (or HSP70h), which is a homolog of the cellular heat shock proteins, p61, and two coat proteins, the major and the minor coat proteins (CP and CPm, respectively). The latter four proteins are involved in virion assembly and also are needed for virus movement along with p6 (Alzhanova et al., 2000; Satyanarayana et al., 2000, 2004; Peremyslov et al., 2004; Tatineni et al., 2010). The remaining five genes that encode p33, p18, p13, p20, and p23 proteins are not found in other members of the *Closteroviridae* (Dawson et al., 2013). Among those, p20 and p23 proteins are absolutely required for infection of plants and have been shown to be involved in suppression of host RNA silencing along with CP (Lu et al., 2004; Tatineni et al., 2008). Three nonconserved proteins, p33, p18, and p13, are dispensable for systemic infection of most *Citrus* spp. CTV mutants with deletions of the corresponding genes are able to infect, multiply, and spread systemically throughout plants of several citrus varieties similarly to the wild type virus (Tatineni et al., 2008). On the other hand, the presence of these genes, and p33 in particular, in the virus genome is required for infection of a few other varieties (Tatineni et al., 2011). Interestingly, the p33 gene product appears to have a major role in extending the virus host range. Thus, acquisition of the p33 gene allowed systemic infection of sour orange, lemon, grapefruit, and calamondin. The products of the other two genes appear to carry out some redundant functions in the latter two hosts: in the absence of p33, p18 permits infection of grapefruit, while p13 allows the virus to infect calamondin (Tatineni et al., 2011).

In addition to extending the ability of CTV to interact with multiple hosts, p33 plays a crucial role in virus superinfection exclusion, a phenomenon in which an initially established viral infection blocks a secondary infection with the same or closely related virus. As we showed recently, mutations within the p33 ORF, which prevented production of the functional protein, resulted in a loss of virus ability to exclude superinfection by the wild type

* Corresponding author.
E-mail address: svetlana@ufl.edu (S.Y. Folimonova).
[1] *Current address*: University of California, Plant Pathology Department, Davis, CA 95616, USA.
[2] *Current address*: Tokyo University of Agriculture, Department of Agriculture, Funako, Atsugi, Kanagawa 243-0034, Japan.

http://dx.doi.org/10.1016/j.virol.2015.03.047
0042-6822/

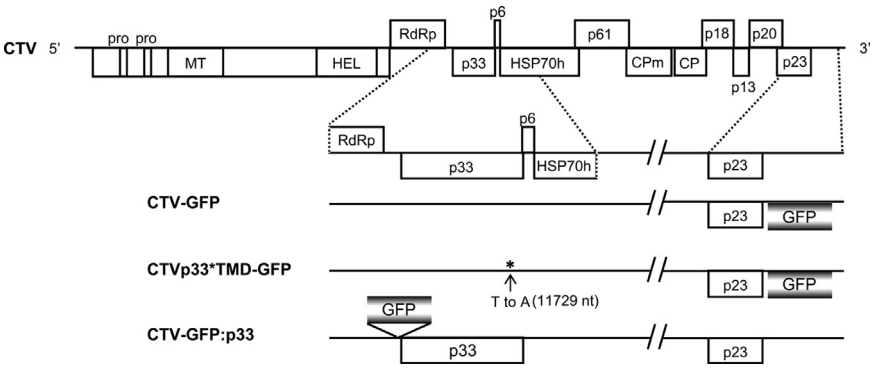

Fig. 1. Schematic representation of the genome of CTV and its derivatives generated in this study. The boxes represent ORFs and their translated products. Pro, papain-like protease domain; MT, methyltransferase; HEL, helicase; RdRp, RNA-dependent RNA polymerase; HSP70h, HSP70 homolog; CPm, minor coat protein; CP, coat protein. The derivatives are shown under the enlarged genome segment. CTV-GFP has GFP ORF inserted between the p23 gene and 3′ NTR of the CTV genome under the native promoter of the CTV CP sgRNA. CTVp33*TMD-GFP has a single nucleotide substitution (T to A) at the position 11,729, which converts the cysteine (C280) codon to a stop codon. CTV-GFP:p33 has the GFP ORF fused to the 5′-terminal end of the p33 gene.

CTV (Folimonova et al., 2010). Moreover, the p33 protein appeared to function in a homology-dependent manner such that its substitution with a cognate protein from a heterologous strain did not confer exclusion, suggesting the existence of precise interactions of p33 with other viral factors involved in this phenomenon (Folimonova, 2012). In spite of an apparent role of p33 in CTV pathogenesis, the protein, however, has not been characterized nor the mechanism of its action is not yet elucidated. The p33 protein appears to be unique and does not share a significant homology with other known proteins, which complicates further understanding of how it functions.

In this study, we examined some of the biochemical properties of the p33 protein along with its subcellular localization. We show that p33 is a membrane protein and is inserted into the membrane via a transmembrane (TM) helix formed by a highly conserved array of hydrophobic amino acid (aa) residues at the C-terminal end. Removal of this TM domain (TMD) dramatically altered the subcellular localization of the protein and also affected virus ability to infect an extended host range.

Results

The p33 protein of CTV contains a putative TMD

Analysis of the aa sequence of the p33 protein encoded in the genome of the T36 isolate of CTV using computer programs MPEx and TMpred (see Materials and methods) revealed presence of a highly hydrophobic region at the C-terminal end of the protein spanning aa residues 279 to 299 (Fig. 2(A)). The protein structure prediction programs, which utilized different algorithms (see Materials and methods), consistently predicted a single α-helical TMD within this hydrophobic region. The free energy for membrane insertion of the predicted TMD based on a biological hydrophobicity scale (Hessa et al., 2005) appeared to be negative enough ($\Delta G_{app} = -1.807$ kcal mol^{-1}) for the protein to be efficiently integrated into the endoplasmic reticulum (ER) membrane by the translocon complex (Woolhead et al., 2004; Elofsson and von Heijne, 2007). Further examination of the aa array of the predicted TMD region by the helix structure analysis tool (http://heliquest.ipmc.cnrs.fr/) showed that all faces of the surface of the TMD helix are uniformly hydrophobic, which suggested that p33 could be tightly inserted into the membrane (data not shown). Interestingly, one of the aromatic residues, tyrosine (Y282), was found toward the N-terminal end of the p33 TMD. Such residues are presumed to be positioned preferably near the end of the membrane-integrated helix and to interact with lipid-water interfacial layer of the membrane (Ulmschneider and Sansom, 2001; Beuming and Weinstein, 2004). No proline residues that could greatly reduce the efficiency of membrane insertion (von Heijne, 1991; Hessa et al., 2005) were found in the p33 TMD. Alignment of the aa sequences of p33 proteins encoded in the genomes of isolates from different CTV strains showed that the TMD region is highly conserved among the cognate proteins of those isolates, with almost identical aa composition (Fig. 2(B)), indicating that membrane insertion of the p33 protein has been preserved in all CTV variants, which could suggest the importance of this region for the protein function.

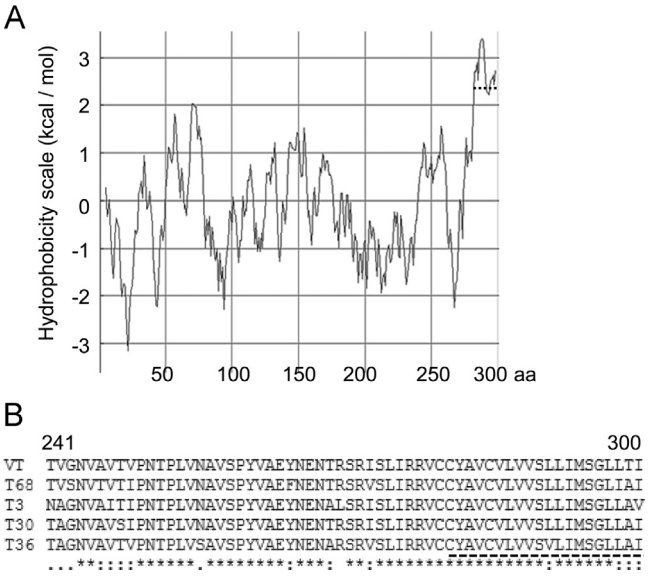

Fig. 2. Analysis of the aa sequence of the p33 protein of CTV. (A) Hydrophobicity plot. Predicted TMD region, which corresponds to the most hydrophobic region, is shown as a dotted line. (B) Alignment of the p33 aa sequences from various strains of CTV. The conserved region matching to the predicted TMD is shown as a dotted line.

p33 is an integral membrane protein

To examine membrane association of p33, we first analyzed protein extracts obtained from *Nicotiana benthamiana* plants, which were infiltrated with *Agrobacterium tumefaciens* culture transformed with a binary vector carrying a fusion of the green fluorescent protein (GFP) gene to the p33 ORF (pGFP:p33) under the 35S

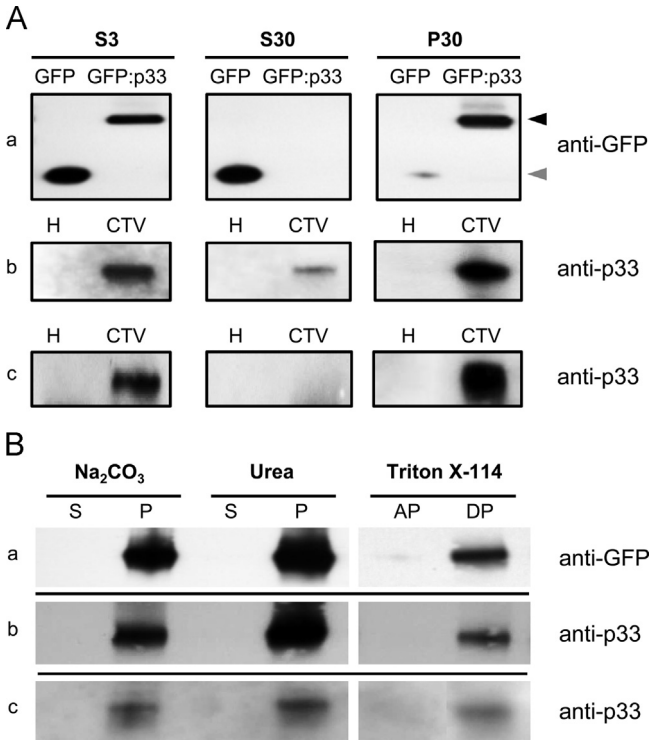

Fig. 3. Subcellular fractionation and immunoblotting analysis of the p33 protein expressed ectopically as a fusion with GFP (GFP:p33) or produced during the course of virus infection as the wild type protein in *N. benthamiana* (a) and (b) or *C. macrophylla* (c). (A) Tissue extracts were subjected to SDS-PAGE followed by immunoblotting using anti-GFP (a) or anti-p33 (b) and (c) antibodies. S3, supernatant following centrifugation of extracts at 3000 × *g*; S30 and P30, supernatant and pellet, following the centrifugation of S3 at 30,000 × *g*, respectively; GFP, plants expressing free GFP; GFP:p33, plants expressing the respective fusion protein; H, healthy, non-inoculated plants; CTV, virus-infected plants. Black triangle pointer indicates the position of the GFP-tagged p33; gray triangle pointer indicates the position of the free GFP. (B) The P30 fractions subjected to treatments with sodium carbonate, urea or Triton X-114 were separated into supernatant ("*S*") and pellet ("*P*") or aqueous ("AP") and detergent ("DP") fractions following centrifugation at 30,000 × *g*. Equivalent amounts of fractions were subjected to SDS-PAGE followed by immunoblotting using anti-GFP (a) or anti-p33 (b) and (c) antibodies.

promoter. Immunoblot analysis of protein extracts subjected to a differential centrifugation at 30,000 × *g* using antibody against GFP showed that GFP:p33 was present exclusively in a pellet fraction (P30), in contrast to the free GFP, which was found mainly in the soluble fraction (S30), with some minor amounts present in the pellet fraction (Fig. 3(A), panel "a"). The fact that the p33 protein was found in the P30 pellet, which represents a crude membrane fraction according to the earlier studies (McKeel and Jarett, 1970; Schaad et al., 1997), suggested that p33 is a membrane-associated protein. To verify whether p33 expressed upon virus infection partitions to the same fraction, we analyzed extracts from *N. benthamiana* and *Citrus macrophylla* plants infected with the wild type CTV. Immunoblot analysis with the antibody generated against p33 showed that the majority of the p33 protein produced upon virus infection was detected in the respective pellet fraction following centrifugation at 30,000 × *g*, similarly to what was found upon *Agrobacterium*-mediated transient expression of the p33 ORF (Fig. 3(A), panels "b" and "c"). To further characterize the association of p33 with membranes, the P30 fractions from each sample were treated with sodium carbonate (pH 11.0), 4 M urea or Triton-X114 in order to determine whether p33 has luminal localization or it is associated with membrane structures. Sodium carbonate treatment, which converts microsomes into open membrane sheets and, therefore, releases soluble luminal proteins (Schaad et al., 1997) did not release the p33 protein into the soluble fraction (Fig. 3(B)). This suggested that p33 is tightly associated with membranes. Furthermore, 4 M urea, which diminishes the hydrophobic interactions by competitive binding to a protein and releases proteins bound to the membrane periphery (Schaad et al., 1997; Reichel and Beachy, 1998), did not release p33 as well, suggesting that the p33 protein is anchored into the membrane (Fig. 3(B)). This was confirmed by the following treatment with Triton X-114. As we expected, upon incubation with Triton X-114, which partitions amphiphilic integral proteins from hydrophilic proteins into a detergent and an aqueous phases, respectively (Bordier, 1981; Mathias et al., 2011), the majority of p33 was detected in the detergent phase, which evidenced that the p33 is an integral membrane protein (Fig. 3(B)).

Upon expression in a host cell p33 localizes to cellular membranous structures

In order to assess the intracellular localization of the p33 protein, *N. benthamiana* leaves expressing GFP:p33 were examined using confocal laser scanning microscopy. The GFP-tagged p33 produced bright fluorescence allowing evaluation of the distribution of the protein inside living cells. The observed distribution of p33 was very distinguishable from that of free GFP (Fig. 4(A) and (B)). As shown in Fig. 4, GFP:p33 localized to the plasma membrane and was also found in the vesicular bodies distributed throughout the cytoplasm, but not in the nucleus (Fig. 4(B) and (C), white arrows), while free GFP appeared to be diffused throughout the cytoplasm and was seen in the nucleus as well (Fig. 4(A)). To show that the observed phenotype of the GFP-tagged p33 is not an artifact due to the protein overexpression driven by the 35S promoter, we generated a construct in which we placed a fusion of the GFP and the p33 genes in the native position of the p33 ORF in the virus genome (CTV-GFP:p33; Fig. 1). Observations of the distribution of the GFP-tagged p33 produced upon virus multiplication in the inoculated leaves of *N. benthamiana* showed that the protein exhibited a phenotype similar to that shown above: the GFP-labeled p33 was found in the association with the plasma membrane as well as in the cytoplasmic vesicular bodies (Fig. 4(D)). The level of GFP:p33 production driven by the native viral promoter in the context of virus infection was slightly less compared to the amount of the protein produced from a 35S promoter-based construct. The similarity of the intracellular distribution of p33 produced under the two conditions validated, however, the use of the 35S promoter-driven expression approach to study the localization and properties of the p33 protein.

CTV p33 is anchored to the membrane via C-terminal TMD

To assess a role of the TMD in p33 association with membrane structures, we generated a construct pGFP:p33ΔTMD in which the GFP ORF was fused to the truncated p33 ORF such that the latter contained a deletion of the 3′-terminal region that codes for the last 25 aa at the C-terminus of the p33 protein (aa 279–303) (Fig. 5(A)). The computer algorithms predicted no putative TMD in the resulted protein, and the calculated free energy value for the membrane insertion was positive, suggesting that this deletion would abolish membrane localization of the protein. To determine whether deletion of the TMD affected the association of p33 with membranes, protein extracts from *N. benthamiana* plants expressing GFP:p33ΔTMD were subjected to a differential centrifugation followed by immunoblot analysis as described above. As we expected, GFP:p33ΔTMD was found only in the soluble fraction (S30) resembling a pattern found with free GFP (Fig. 5(B)), in a contrast to the GFP-tagged wild type p33, which as we showed above, partitioned to the pellet fraction (Fig. 3 (A)). The subcellular localization of the mutant p33 lacking the TMD significantly differed from that of the parental protein. The fluorescence of GFP:p33ΔTMD was observed throughout the cytoplasm and

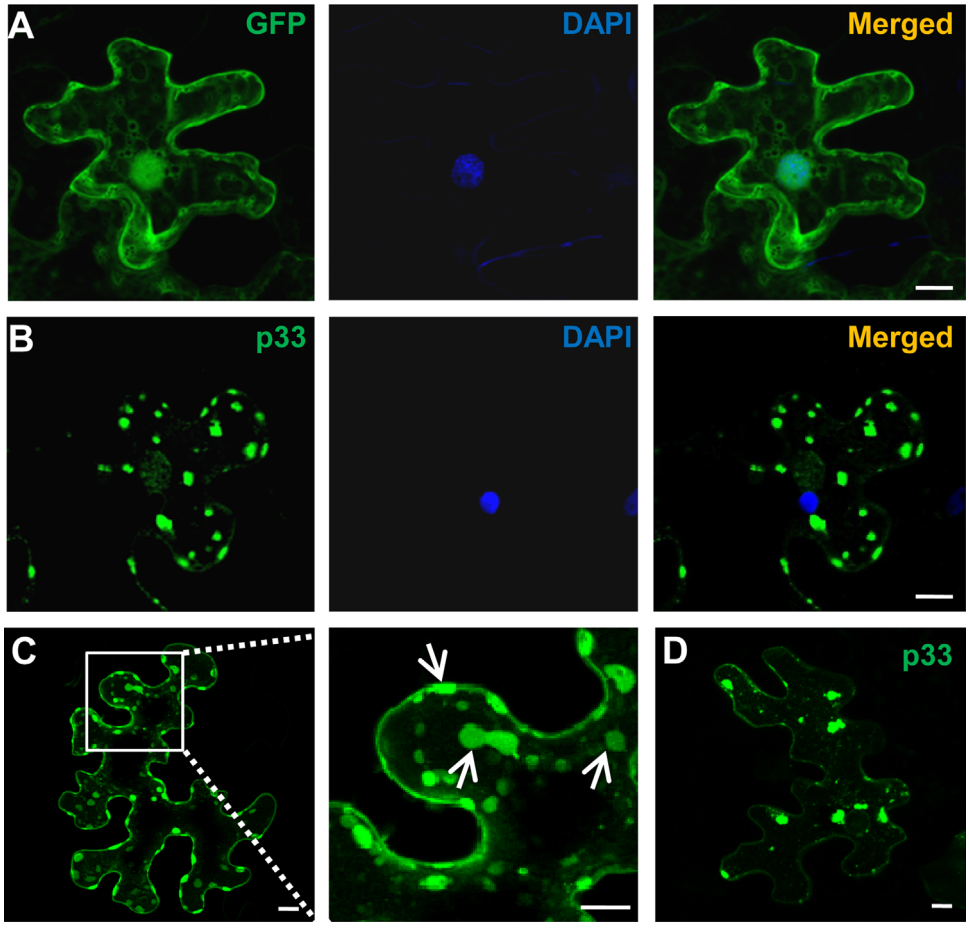

Fig. 4. Subcellular localization of the p33 protein. Images show confocal projections of *N. benthamiana* leaves agroinfiltrated with the following constructs: (A) pGFP, (B) and (C) pGFP:p33, (D) pCTV-GFP:p33. Cell shown in images A and B were stained with DAPI. The white arrows in the enlarged image (C) show accumulation of the GFP-tagged p33 at the plasma membrane and in the cytoplasmic vesicular structures. Scale bars, 10 μm.

in the nucleus, similar to that produced by free GFP (Fig. 5(B)). No vesicle-like structures characteristic of the wild type p33 (Fig. 4(B) and (C)) were found with the p33ΔTMD mutant. These observations along with the results of the immunoblot analyses indicated that the deletion of the TMD completely abolished membrane association of the p33 protein.

In addition to the assays described above, we examined whether the TMD of p33 alone is capable of targeting another unrelated protein to the cellular membranes. In order to address this question, a sequence of the TMD was fused to the 3′ terminus of the GFP ORF (Fig. 5(A); pGFP:TMD). Another construct was created by fusing the GFP ORF with a mutated version of the TMD, SPTMD, carrying substitutions of each of the two serines at the aa positions 290 and 295 with the proline (Fig. 5(A); pGFP:SPTMD). Such mutations were expected to distort the membrane-spanning α-helix by disrupting the direction of the peptide chain due to the cyclic structure of prolines (Deber and Therien, 2002; Genovés et al., 2011). Immunoblot analysis of the protein extracts obtained from infiltrated leaves using anti-GFP antibody showed that unlike free GFP the fusion of GFP to the TMD partitioned to the crude fraction of cellular membranes, P30 (Fig. 5(B)). In contrast, as we expected, a significant proportion of GFP:SPTMD was found in the soluble fraction (Fig. 5(B)), suggesting that membrane association conferred by the TM α-helix was affected by the respective change in its topology. Examination of the subcellular localization of the engineered fusion proteins revealed that their distribution was distinct from that of the parental GFP. GFP:TMD was found exclusively along the plasma membrane confirming the ability of the TMD of p33 target unrelated proteins to the membrane (Fig. 5(B)), whereas GFP:SPTMD was evenly distributed in the cytoplasm similarly to GFP:p33ΔTMD, with some fluorescence seen on the cellular membrane (Fig. 5(B)). These observations, along with the findings presented above, confirmed that the predicted hydrophobic α-helix at C-terminal end of p33 has a key role in anchoring the protein to the membrane.

Membrane association of p33 confers virus ability to infect an extended host range

Previously, it has been demonstrated that mutants of CTV that have a deletion of the p33 ORF were unable to infect certain citrus hosts (Tatineni et al., 2011). To examine whether membrane association of the p33 protein is important for the ability of CTV to establish infection in an extended host range, we generated a CTV variant, which produced the TMD-less version of p33 (CTVp33*TMD-GFP; Fig. 1). This virus variant had also the GFP ORF inserted in the genome as an extra gene, which allowed monitoring of virus accumulation in the inoculated plants. While engineering the viral construct, we avoided deleting the whole nucleotide sequence encoding the p33 TMD region. This sequence represents a part of the promoter for the sgRNA that serves as mRNA for translation of the p6 protein, for which ORF is positioned downstream of the p33 ORF (Fig. 1) (Ayllón et al., 2005). Instead, CTVp33*TMD-GFP was generated by introducing a single nucleotide substitution (TG*T* to TG*A*) converting the codon for the cysteine, positioned at the beginning of the predicted TMD, at the aa position 280 into a stop

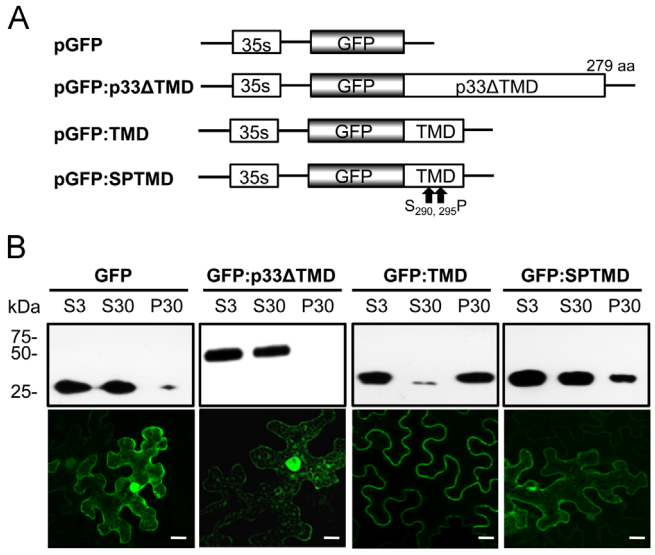

Fig. 5. The TMD of p33 confers membrane association of the protein. (A) Schematic diagram of constructs used in this study. pGFP:p33ΔTMD encodes the GFP-tagged truncated p33 that lacks TMD. GFP:TMD encodes fusion of GFP with the p33 TMD encompassing C-terminal aa residues 279–303. GFP:SPTMD encodes fusion of GFP with the TMD carrying mutations S_{290}P and S_{295}P. (B) Protein extracts obtained from *N. benthamiana* plants expressing free GFP, GFP:p33ΔTMD, GFP:TMD or GFP:SPTMD were subjected to the differential centrifugation as shown in Fig. 3. Fractions were subjected to SDS-PAGE followed by immunoblotting using anti-GFP antibody. S3, supernatant following extract centrifugation at 3000 × *g*; S30 and P30, supernatant and pellet, respectively, following centrifugation of S3 at 30,000 × *g*. The bottom panel shows confocal projections of mesophyll cells of *N. benthamiana* leaves agroinfiltrated with the respective constructs. Scale bars, 10 μm.

codon. Immunoblot analysis of protein extracts obtained from *N. benthamiana* plants inoculated with CTVp33*TMD-GFP demonstrated the presence of the truncated p33 protein lacking the TMD exclusively in the fraction of soluble proteins (Fig. 6(A)), in contrast to the full-length p33 produced upon infection with the wild type CTV, which partitions into the fraction of cellular membranes as we demonstrated above (Fig. 3(A), panel "b"). As the next step, CTVp33*TMD-GFP was used for inoculation of a series of *C. macrophylla* and sour orange plants. As a control in this experiment, a set of plants of the same two varieties was inoculated with the GFP-tagged wild type CTV (Fig. 1; CTV-GFP). As a result in this experiment, both virus variants successfully established systemic infections in *C. macrophylla* plants, which was confirmed by ELISA assays using CTV-specific antiserum (Fig. 6(B)) and by observation of GFP fluorescence produced upon multiplication of the viruses in the inoculated trees (data not shown). Furthermore, sour orange plants inoculated with CTV-GFP showed virus infection as well (Fig. 6(B)). The titer of CTV-GFP in plants of this citrus variety was lower than that found in *C. macrophylla* plants, which was in the agreement with the previous observations showing that sour orange is less susceptible to infection by CTV (Folimonova et al., 2008). At the same time, sour orange plants inoculated with CTVp33*TMD-GFP remained virus-free, which was confirmed by ELISA assays and lack of GFP fluorescence in the inoculated plants (Fig. 6(B) and data not shown). The virus variant expressing the p33 protein lacking the TMD was unable to infect this citrus variety. Such behavior was similar to that of the virus mutant containing a deletion of the p33 ORF, which also could not infect sour orange (Tatineni et al., 2011).

As an alternative strategy to examine the ability of CTVp33*TMD-GFP to infect sour orange, we used an approach that was successfully utilized by us and other researchers for the analysis of susceptibility of different citrus varieties to variants of CTV in the earlier studies (Folimonova et al., 2008; Tatineni et al., 2011). Small rectangular areas of bark from the stems of *C. macrophylla* trees infected with CTVp33*TMD-GFP or CTV-GFP were replaced with bark patches of an equal size excised from healthy sour orange or *C. macrophylla* trees. The plants were further maintained for ten weeks to allow the substituted bark patches to establish vascular connections. The examination of the junction areas of the grafted bark patches using a fluorescence microscope showed that in all sets the bark tissue of *C. macrophylla* trees appeared to be heavily infected (Fig. 6(C)). Abundant GFP fluorescence was also observed in the *C. macrophylla* patches placed into the CTVp33*TMD-GFP- and CTV-GFP-infected trees, showing that the virus was able to successfully infect the introduced tissue patches (Fig. 6(C)). Significant amount of GFP fluorescence was observed in the sour orange patches placed into the trees infected with the GFP-tagged wild type CTV (Fig. 6(C)). However, no GFP fluorescence was detected in the sour orange patches grafted into the CTVp33*TMD-GFP-infected trees (Fig. 6(C)). This result demonstrated that a CTV variant, which produces a truncated p33 protein lacking the TMD, acts as a previously described mutant containing a deletion of the p33 protein gene, which also was unable to infect sour orange variety (Tatineni et al., 2008, 2011) and suggested that membrane association of p33 conferred by its C-terminal TMD is important for virus ability to infect an extended host range.

Discussion

Previous studies have shown that the p33 protein of CTV plays an important role in the virus pathogenesis. The protein is encoded only in the genomes of CTV isolates and has no significant homology with other known proteins. To some extent, the uniqueness of p33 could account for the lack of understanding of the modes of action of this protein. In this work, we examined some of the characteristics of the p33 protein along with its intracellular localization. We show that p33 is a membrane-associated protein and is inserted into the membrane via a TMD positioned at its C-terminal end. Immunoblotting assay of protein extracts obtained from plants expressing p33 showed that p33 partitioned exclusively to the fraction containing cellular membranes. A series of chemical treatments applied to this fraction confirmed that the protein is tightly associated with the membrane. Microscopic observations of plant cells expressing the GFP-tagged p33 revealed that the p33 protein accumulates at the plasma membrane and also forms cytoplasmic vesicles. Furthermore, the C-terminal TMD appeared to play a key role in anchoring p33 to the membrane. A p33 mutant containing a deletion of TMD lost membrane targeting and was seen dispersed throughout the cytoplasm similarly to free GFP. Moreover, the TMD alone was able to convey the tagged GFP to the membrane as was demonstrated by the analysis of the fractionated protein extracts from plants expressing GFP:TMD fusion and by the observation of its intracellular distribution.

The subcellular localization of a protein with a TMD is determined by the length, hydrophobicity, and the aa composition of the TMD sequence (Brandizzi et al., 2007; Thomas et al., 2008). The length of the TMD of p33 appears to be similar to that of TMDs of other plant viral proteins targeted to the cellular membranes (Schaad et al., 1997; Han and Sanfaçon, 2003; Peremyslov et al., 2004; Liu et al., 2005; McCartney et al., 2005; Martínez-Gil et al., 2010; Genovés et al., 2011). Indeed, GFP:TMD was localized almost exclusively to the membrane, thus suggesting that TMD of p33 has an adequate length to confer its membrane anchoring property. Double-substitution mutations (Ser to Pro) introduced in the middle of the TMD region altered the free energy value for a predicted membrane insertion ($\Delta G_{app} = -1.118$ kcal mol^{-1}). This was correlated with a change in the subcellular localization of the resulted mutant: a significant amount of GFP:SPTMD was found in the fraction of soluble proteins, indicating that the introduction of prolines substantially affected the topology of p33 TMD. The effect

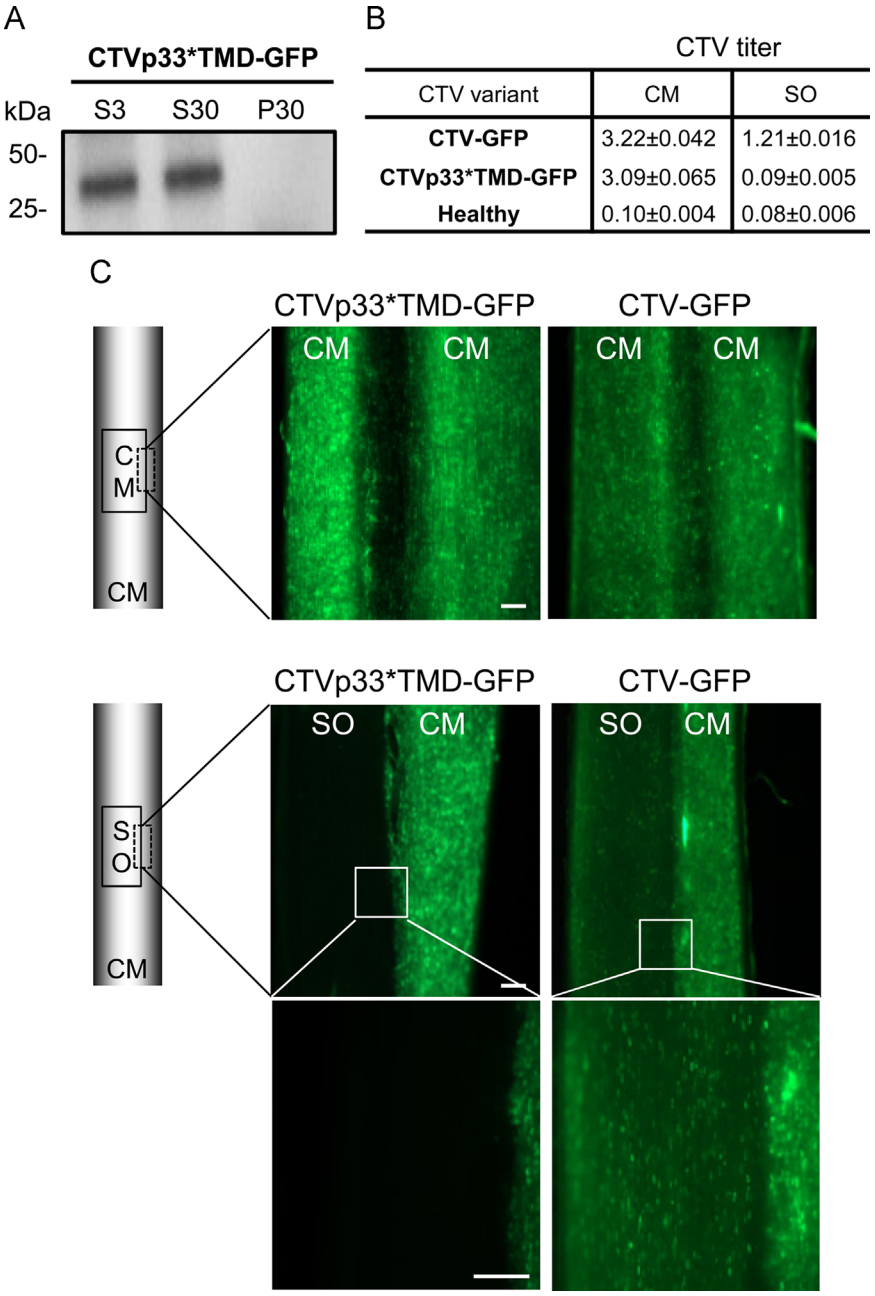

CTV variant	CM	SO
CTV-GFP	3.22±0.042	1.21±0.016
CTVp33*TMD-GFP	3.09±0.065	0.09±0.005
Healthy	0.10±0.004	0.08±0.006

Fig. 6. Examination of CTVp33*TMD-GFP infection in *C. macrophylla* and sour orange. (A) Immunoblot analysis showing partitioning of the truncated p33 produced by GFPp33*TMD-GFP in *C. macrophylla* following differential centrifugation of the corresponding protein extracts. (B) Examination of virus titer in *C. macrophylla* and sour orange plants inoculated with CTV-GFP or CTVp33*TMD-GFP. Analysis was done at twelve weeks after inoculation using ELISA with CTV-specific antibody. CTV titers (A_{405} values obtained by ELISA) are averages of the results for 5 plants, three wells per plant. (C) Detection of GFP fluorescence in the junction of bark patch. Small rectangular areas of bark from the stems of *C. macrophylla* trees infected with CTVp33*TMD-GFP or CTV-GFP were replaced with bark patches of an equal size excised from healthy sour orange or *C. macrophylla* trees. Examination was done at ten weeks post grafting. CM, *C. macrophylla*; SO, sour orange. Scale bars, 0.3 mm.

of such substitution is likely to be due to the position of the mutated residues, which are located in the center of the α-helix structure (Hessa et al., 2005). A similar situation was reported for the membrane-associated movement protein of *Melon necrotic spot virus*, which also has a single-pass TMD: a proline residue introduced into the middle of the TMD sequence was shown to affect the localization as well as the function of the protein (Genovés et al., 2011).

Membrane association of proteins produced by viruses during the viral cycle is common. Often such association prompts rearrangement of the cellular membranous structures resulting in the formation of vesicular bodies, which offer a protected and favorable environment for virus replication, translation, virion assembly as well as intra- and intercellular virus movement (reviewed in Laliberté and Zheng, 2014). Thus, many viral proteins involved in virus replication and/or movement were shown to associate with and remodel the cellular membranes. Some examples are P1 and P2 of *Alfalfa mosaic virus* (AMV) (van Der Heijden et al., 2001), 1a and 2a of *Brome mosaic virus* (Restrepo-Hartwig and Ahlquist, 1999), RNA 1-encoded proteins of *Cowpea mosaic virus* and *Grapevine fanleaf virus* (GFLV) (Carette et al., 2000; Ritzenthaler et al., 2002), p27 and p88 proteins of *Red clover necrotic mosaic virus* (RCNMV) (Turner et al., 2004) and NTB protein of *Tomato ringspot virus* (Han and Sanfaçon, 2003), which were shown to confer virus genome replication in the association with cellular membranous structures. Many movement-related proteins are particularly

known to associate with membranes (reviewed in Harries et al., 2010). Thus, the AMV MP (Huang and Zhang, 1999), 37 kDa protein of *Chinese wheat mosaic virus* (Andika et al., 2013), GFLV MP (Laporte et al., 2003), the triple gene block proteins of *Potato virus X* (Krishnamurthy et al., 2003; Mitra et al., 2003; Ju et al., 2005), RCNMV MP (Kaido et al., 2011), *Turnip crinkle virus* p9 protein (Martínez-Gil et al., 2010), *Tobacco etch virus* (TEV) 6 kDa protein (Schaad et al., 1997), $6K_2$ protein of *Turnip mosaic virus* (Grangeon et al., 2012), and *Tobacco mosaic virus* 30 K MP (Heinlein et al., 1998) are a few examples. The membrane association of proteins encoded by viruses from the family *Closteroviridae* is less studied. The Hsp70h and the p6 movement protein of *Beet yellow virus* (BYV), a type species of the genus *Closterovirus*, were reported to localize to the ER membrane, and both were shown to play roles in facilitating cell-to-cell movement of BYV (Medina et al., 1999; Peremyslov et al., 2004). Also, the p34 protein encoded by *Lettuce infectious yellows virus,* a member of the genus *Crinivirus*, shown to be an enhancer of RNA 2 replication, was reported to colocalize with the ER including the perinuclear region (Yeh et al., 2000; Wang et al., 2010). Apparently, the p33 protein is not needed for replication since the virus lacking the respective gene is able to efficiently multiply in the transfected protoplasts as well as to infect a number of citrus varieties (Tatineni et al., 2008). On the other hand, p33 was shown to be required for systemic infection of a few specific hosts, including sour orange, which led to a hypothesis that the protein could facilitate CTV movement in certain species (Tatineni et al., 2011). As we demonstrated in this work, membrane insertion of p33 was critical for the ability of the virus to infect sour orange variety, which suggests that association of this viral protein with the cellular membranes plays a vital role in mediating systemic infection in the latter and, possibly, the other hosts for which the presence of p33 is essential.

The p33 protein is not conserved among other closteroviruses. Interestingly, though, a few viruses in the genus *Closterovirus* have an extra gene at the same genomic position as the p33 gene of CTV. So far, three such genes were identified: the p25 gene of *Rose leaf rosette-associated virus*, the p30 gene of *Beet yellow stunt virus*, and the p28 gene of *Strawberry chlorotic fleck-associated virus* are all positioned between the ORF 1b, which encodes RNA-dependent RNA polymerase, and the ORF encoding the orthologs of p6 (He et al., 2014). No significant similarity was found between the four proteins, and none of them shows homology with other known proteins. On the other hand, they all appear to possess a C-terminal TMD. More interestingly, not only the length of the predicted TMDs is similar but also the aa sequences of TMD regions display up to 61% similarity (Tzanetakis and Martin, 2007; He et al., 2014). Therefore, it would not be unreasonable to propose that those genes had been acquired by these viruses in the course of their adaptation to the environment for the same purpose, which, possibly, is to extend the range of their hosts. Further research is needed to identify the function(s) of these proteins in virus infection as well as to gain a better understanding of the genome complexity of large plant RNA viruses like CTV and other closteroviruses.#

Materials and methods

In silico sequence analysis

Hydrophobicity plot was analyzed using MPEx (Wimley and White, 1996) (http://blanco.bio.mol.uci.edu/mpex/) and TMpred (Hofmann and Stoffel, 1993) (http://www.ch.embnet.org/software/TMPRED_form.html/) and generated using ProtScale on ExPASy (Kyte and Doolittle, 1982; http://web.expasy.org/protscale/). The prediction of TM helices was performed with Genesilico Fold Prediction Metaserver (https://www.genesilico.pl/meta2/) and InterPro (http://www.ebi.ac.uk/interpro/). The free energy value for membrane insertion was estimated using ΔG predictor (Hessa et al., 2005) (http://dgpred.cbr.su.se/). The physiochemical property of the predicted TM helix was analyzed using HeliQuest (http://heliquest.ipmc.cnrs.fr/). The p33 sequences of the type isolates of the T36 (EU937521), VT (EU937519), T68 (JQ965169), T3 (KC525952), and T30 (EU937520) strains were aligned with ClustalX 1.83 (Thompson et al., 1997) and viewed with GeneDoc software (Nicholas et al., 1997).

Generation of constructs for transient expression of GFP-tagged p33 or its fragments in plants

The pGFP:p33, pGFP:p33ΔTMD, pGFP:TMD, and pGFP:SPTMD constructs were created by an overlap-extension polymerase chain reaction (OE-PCR) using two PCR fragments, one containing a fusion of the 5′ non-translated region (NTR) of TEV (Carrasco et al., 2007) to the GFP ORF and the other containing the complete or truncated ORF of p33, which were generated as described below. The first product, TEV-GFP fragment, was generated by fusing the 5′ NTR of TEV in front of the GFP ORF using PCR with oligonucleotides C-1728 (AACACAACATATACAAAACAAACGAAT) and C-2169 (TTCGCTCGCGAAGGCAAACATTTTGTAGAGCTCATCCATGCCATG). The full-length cDNA clone of CTV (CTV-GFP) in the binary vector pCAMBIA-1380 (Satyanarayana et al., 1999, 2001; Gowda et al., 2005; El-Mohtar and Dawson, 2014) was used to amplify the ORF of the wild type p33 or the different fragments of the latter ORF (p33ΔTMD, TMD or SPTMD) using PCR with oligonucleotides C-2168 (GGCATGGATGAGCTCTACAAAATGTTTGCCTTCGCGAGCGAAAGC) and C-2170 (ATTGGTACCTCATATAAATATAATGGCTAATAAACCGCTCATTAT) to amplify the p33 ORF, C-2168 and C-2170ΔTMD (ATTGGTACCTCAGCGTATTAATGAGACGCGCGAGCGTGCATTCTC) to amplify p33ΔTMD, C-2168 and SHK-129 (GACAATGGTACC TCATATAAATATAATGGCTAATAAACCGCTCATTATAAGAACGGACACCAC-TAAAACGCAAACGGCGTAACAACAGACCCGTTTGTAGAGCTCATCCATGC-CATG) to amplify TMD, C-2168 and SHK-142 (GACAATGGTACC TCATATAAATATAATGGCTAATAAACCGGGCATTATAAGAACGGGCACCAC-TAAAACGCAAACGGCGTAACAACAGACCCGTTTGTAGAGCTCATCCATGC-CATG) to amplify SPTMD. The OE-PCR was performed using C-1728 and C-2170 to create pGFP:p33, C-1728 and C-2170 to create pGFP:p33ΔTMD, C-1728 and SHK-129 to create pGFP:TMD, C-1728 and SHK-142 to create pGFP:SPTMD. The PCR products were digested with *Kpn*I restriction endonuclease. The digested products were substituted for the corresponding fragment in the pCASS-4N plasmid, which was also digested with *Stu*I (generating a blunt end at the position of the 5′ end insertion) and *Kpn*I restriction endonucleases.

*Generation of pCTVp33*TMD-GFP*

pCTVp33*TMD-GFP carrying a single nucleotide substitution introducing a stop codon in front of the sequence encoding TMD of p33 was generated using a primer embedding the substitution. Two PCR products were generated using a set of oligonucleotides C-FW8100 (GGGTTGGTTCCTTGCCCGGGTTCTCAGAAATATGATTATGCTTTG) and C-P33sRV (CTAAAACGCAAACGGCGTAACATCAGACCCGGCGTATTAATGAGAC) and another set of oligonucleotides C-P33sFW (GTCTCATTAATACGCCGGGTCTGATGTTACGCCGTTTGCGTTTTAG) and C-RV11900 (CAGTCCATTAAACCCCGTTTAAACAGAGTCAAACGGCGAGTCTTAAG). The two products were used to generate OE-PCR product using C-FW8100 and C-RV11900, which was subsequently digested with *Xma*I and *Pme*I restriction endonucleases. The digested fragment with the stop codon was substituted for the corresponding fragment of pCTV-GFP, which was digested with the same enzymes (*Xma*I and *Pme*I).

Generation of pCTV-GFP:p33

The GFP ORF was fused to the 5′ end of the p33 ORF in the CTV genome. Two PCR products were generated by using a set of oligonucleotides SHK-122 (GTTGGTTCCTTGCCCGGGTTCTCAG) and SHK-123 (AAGTTCTTCTCCTTTGCTAGCCATCCTGACTCAACTACCCACATTAGC) and another set of oligonucleotides SHK-124 (AGAGCTAATGTGGGTAGTTGAGTCAGGATGGCTAGCAAAGGAGAAGAACTTTTC) and SHK-125 (CATTAAACCCCGTTTAAACAGAGTCAAACGGCGAGTCTTAAGTAAGTAATTGTACCTTATGAGTTACTACACTAAATCATATAAATATAATGGCTAATAAACC). The two products were used to generate OE-PCR product using SHK-122 and SHK-125, which was subsequently digested with *Xma*I and *Pme*I restriction endonucleases. The digested fragment was substituted for the corresponding fragment of the wild type CTV digested with the same enzymes.

Agroinfiltration of CTV constructs into N. benthamiana

Agroinfiltration of constructs was conducted as previously described (Ambrós et al., 2011; El-Mohtar and Dawson, 2014). Briefly, plasmids were introduced by heat shock into *A. tumefaciens* EHA105, and the resulting transformants were selected on the Luria–Bertani agar plates containing two antibiotics (50 mg/ml rifampicin and 25 mg/ml kanamycin). Cells collected from an overnight culture of a selected single colony were gently resuspended in a buffer containing 10 mM 2-(N-morpholino) ethane sulfonic acid (MES, pH 5.85), 10 mM $MgCl_2$ and 150 mM acetosyringone at $O.D._{600nm}=1.0$. Following three-hour incubation at room temperature without shaking the suspension was infiltrated into three-weeks-old *N. benthamiana* plants using needless syringe.

Virus purification and inoculation of citrus trees

CTV virions were purified from leaves of *N. benthamiana* plants infected with CTVp33*TMD-GFP and CTV-GFP by ultra-centrifugation using sucrose cushion and used for inoculation of one year-old *C. macrophylla* plants as described previously (Robertson et al., 2005). CTVp33*TMD-GFP and CTV-GFP have been further maintained in the citrus plants under greenhouse condition along with plants infected with the wild type CTV (Folimonova et al., 2010). These plants were used for subsequent graft inoculations of additional receptor trees as described (Folimonova et al., 2010). Retention of the introduced single-nucleotide mutation by CTVp33*TMD-GFP multiplying in the inoculated citrus was confirmed by sequencing the DNA fragments obtained by reverse transcription-PCR using nucleic acid extracts from the infected plants and oligonucleotide primers amplifying the p33 ORF. When the graft healed, the upper flushes of leaves were trimmed to induce growth of a new flush, which was then evaluated for the ability of virus to establish infection in plants.

Production of anti-p33 antibody

Three regions of the p33 aa sequence were selected for anti-peptide antibody production (15–33 aa: KWFRRRTYHRKYFGDVVKD, 185–199 aa: SVATDDVEDVKYIRK, and 264–280 aa: EYNENARSRVSLIRRVC) based on the hydrophilicity plot. Custom antibody production using rabbits was completed by Genemed Synthesis Inc. (San Antonio, TX, USA).

Subcellular fractionation and immunoblotting analysis

Both *N. benthamiana* and *C. macrophylla* samples were ground in a lysis buffer (50 mM Tris–HCl, 1 mM EDTA, 150 mM NaCl, 5% glycerol) containing protease inhibitor cocktail (AEBSF, Bestatin, E-64, Leupeptin, Pepstatin A and 1,10-Phenanthroline; SIGMA), and the homogenate was clarified by centrifugation at 3000 × *g* for 10 min at 4 °C. The supernatant (S3) was centrifuged again at 30,000 × *g* for 30 min at 4 °C to separate the soluble (S30) and the microsomal (P30) fractions. The P30 fractions were resuspended in 0.1 M Na_2CO_3 (pH 11.0) or 4 M urea followed by incubation on ice for 30 min. The soluble (S30) and membrane-enriched pellet (P30) fraction were separated by centrifugation at 30,000 × g for 30 min at 4 °C, then the pellet was resuspended in the lysis buffer. Treatment of P30 with Triton X-114 was performed separately. The P30 fraction was resuspended in the lysis buffer containing 1% Triton X-114 followed by incubation on ice for 30 min. Mixture was clarified by centrifugation at 10,000 × *g* for 20 min at 4 °C, then the supernatant was incubated at 37 °C for 10 min followed by subsequent centrifugation at 5000 × *g* for 10 min at room temperature to separate the aqueous and the hydrophobic phase. The hydrophobic, detergent-enriched fraction was mixed with the lysis buffer. For immunoblot analysis, all fractions were mixed with the equal volume of the 2X sample loading buffer (125 mM Tris–HCl, 4% SDS, 20% glycerol, and 0.01% bromophenol blue) with dithiothreitol and boiled for 10 min. Mixtures were briefly centrifuged prior to loading and electrophoresed through 10% SDS-polyacrylamide gels and electro-transferred to polyvinylidene difluoride membrane. The membrane was blocked with 1X TBS-T (137 mM NaCl, 27 mM KCl, 250 mM Tris–HCl, and 1% Tween-20) containing 5% (w/v) skim milk for an hour at room temperature prior to be probed by anti-GFP (dilution: 1:1000; Santa Cruz Biotechnology) or anti-p33 antibody (dilution: 1:500) with 1X TBS-T for another hour. Anti-rabbit IgG conjugated to horseradish peroxidase was used as a secondary antibody (dilution: 1:20,000; Santa Cruz Biotechnology), and the signal was visualized on chemiluminescence film (X-OMAT LS) in a dark room (Carestream Kodak, Sigma-Aldrich, USA).

Serological assays

Double-antibody sandwich ELISA of tissue extracts was performed as described previously (Folimonova, 2012) to confirm the infection of primary infection. Briefly, 0.25 g of citrus bark tissue was ground in 5 ml of the extraction buffer per sample. Purified IgG from rabbit polyclonal antiserum CTV-908 (1 ug/ml) was used as a coating antibody, then a broadly reactive CTV monoclonal antibody, ECTV172, was used for detection.

Examination of fluorescence in citrus plants infected with GFP-tagged CTV

Bark tissues from trees inoculated with CTVp33*TMD-GFP or CTV-GFP were examined for GFP fluorescence at ten weeks after graft-inoculation using a Leica MZ 10F UV fluorescence dissecting microscope (Leica Micro- systems, Bannockburn, IL, USA).

DAPI staining

N. benthamiana leaves were cut in small pieces and dipped in 10 ug/ml of 4′,6-diamidino-2-phenylindole (DAPI) solution (Sigma-Aldrich) for two hours at room temperature.

Laser-scanning confocal microscopy

Mesophyll cells of *N. benthamiana* leaves were observed after four days post-infiltration using Leica TCS SP5 confocal laser scanning microscope system (Leica Micro-systems, Bannockburn, IL, USA). GFP fluorescence was detected with excitation at 488 nm and emission capture at 490–530 nm. The DAPI was excited with a 405 nm laser, and emission was collected from 405–500 nm. Images were captured using a 20 × objective or a 63 × oil-immersion objective.

Acknowledgments

This research was supported by the National Science Foundation under Grant no. 1050883 (to S.Y. Folimonova). Any opinions, findings, and conclusions or recommendations expressed in this material are those of the author(s) and do not necessarily reflect the views of the National Science Foundation.

Appendix A. Supporting information

Supplementary data associated with this article can be found in the online version at http://dx.doi.org/10.1016/j.virol.2015.03.047.

References

Agranovsky, A.A., 1996. Principles of molecular organization, expression, and evolution of closteroviruses: over the barriers. Adv. Virus Res. 47, 119–158. http://dx.doi.org/10.1016/S0065-3527(08)60735-6.

Alzhanova, D.V., Hagiwara, Y., Peremyslov, V.V., Dolja, V.V., 2000. Genetic analysis of the cell-to-cell movement of beet yellows closterovirus. Virology 268 (1), 192–200. http://dx.doi.org/10.1006/viro.1999.0155.

Ambrós, S., El-Mohtar, C., Ruiz-Ruiz, S., Peña, L., Guerri, J., Dawson, W.O., Moreno, P., 2011. Agroinoculation of *Citrus tristeza* virus causes systemic infection and symptoms in the presumed nonhost *Nicotiana benthamiana*. Mol. Plant–Microbe Interact. 24, 1119–1131. http://dx.doi.org/10.1094/MPMI-05-11-0110.

Andika, I.B., Zheng, S., Tan, Z., Sun, L., Kondo, H., Zhou, X., Chen, J., 2013. Endoplasmic reticulum export and vesicle formation of the movement protein of Chinese wheat mosaic virus are regulated by two transmembrane domains and depend on the secretory pathway. Virology 435, 493–503. http://dx.doi.org/10.1016/j.virol.2012.10.024.

Ayllón, M.A., Satyanarayana, T., Gowda, S., Dawson, W.O., 2005. An atypical 3′-controller element mediates low-level transcription of the p6 subgenomic mRNA of *Citrus tristeza* virus. Mol. Plant Pathol. 6, 165–176. http://dx.doi.org/10.1111/J.1364-3703.2005.00275.X.

Bar-Joseph, M., Garnsey, S.M., Gonsalves, D., 1979. The closteroviruses: a distinct group of elongated plant viruses. Adv. Virus Res. 25, 93–168. http://dx.doi.org/10.1016/S0065-3527(08)60569-2.

Beuming, T., Weinstein, H., 2004. A knowledge-based scale for the analysis and prediction of buried and exposed faces of transmembrane domain proteins. Bioinformatics 20, 1822–1835. http://dx.doi.org/10.1093/bioinformatics/bth143.

Bordier, C., 1981. Phase separation of integral membrane proteins in Triton X-114 solution. J. Biol. Chem. 256, 1604–1607.

Brandizzi, F., Frangne, N., Marc-Martin, S., Hawes, C., Neuhaus, J., Paris, N., 2007. The destination for single-pass membrane proteins is influenced markedly by the length of the hydrophobic domain. Plant Cell 14, 1077–1092. http://dx.doi.org/10.1105/tpc.000620.

Carette, J.E., Stuiver, M., van Lent, J., Wellink, J., van Kammen, A., 2000. Cowpea mosaic virus infection induces a massive proliferation of endoplasmic reticulum but not Golgi membranes and is dependent on de novo membrane synthesis. J. Virol. 74, 6556–6563. http://dx.doi.org/10.1128/JVI.74.14.6556-6563.2000.

Carrasco, P., Daròs, J.A., Agudelo-Romero, P., Elena, S.F., 2007. A real-time RT-PCR assay for quantifying the fitness of tobacco etch virus in competition experiments. J. Virol. Methods 139, 181–188. http://dx.doi.org/10.1016/j.jviromet.2006.09.020.

Dawson, W.O., Garnsey, S.M., Tatineni, S., Folimonova, S.Y., Harper, S.J., Gowda, S., 2013. *Citrus tristeza* virus–host interactions. Front. Microbiol 4, 88. http://dx.doi.org/10.3389/fmicb.2013.00088.

Deber, C.M., Therien, A.G., 2002. Putting the beta-breaks on membrane protein misfolding. Nat. Struct. Biol. , http://dx.doi.org/10.1038/nsb0502-318.

Dolja, V.V., Karasev, A.V., Koonin, E.V., 1994. Molecular biology and evolution of closteroviruses: sophisticated build-up of large RNA genomes. Annu. Rev. Phytopathol. 32, 261–285.

Dolja, V.V., Kreuze, J.F., Valkonen, J.P.T., 2006. Comparative and functional genomics of closteroviruses. Virus Res. 117, 38–51. http://dx.doi.org/10.1016/j.virusres.2006.02.002.

El-Mohtar, C., Dawson, W.O., 2014. Exploring the limits of vector construction based on *Citrus tristeza* virus. Virology 448, 274–283. http://dx.doi.org/10.1016/j.virol.2013.10.017.

Elofsson, A., von Heijne, G., 2007. Membrane protein structure: prediction versus reality. Annu. Rev. Biochem. 76, 125–140. http://dx.doi.org/10.1146/annurev.biochem.76.052705.163539.

Folimonova, S.Y., 2012. Superinfection exclusion is an active virus-controlled function that requires a specific viral protein. J. Virol. 86, 5554–5561. http://dx.doi.org/10.1128/JVI.00310-12.

Folimonova, S.Y., Folimonov, A.S., Tatineni, S., Dawson, W.O., 2008. *Citrus tristeza* virus: survival at the edge of the movement continuum. J. Virol. 82, 6546–6556. http://dx.doi.org/10.1128/JVI.00515-08.

Folimonova, S.Y., Robertson, C.J., Shilts, T., Folimonov, A.S., Hilf, M.E., Garnsey, S.M., Dawson, W.O., 2010. Infection with strains of *Citrus tristeza* virus does not exclude superinfection by other strains of the virus. J. Virol. 84, 1314–1325.

Genovés, A., Pallás, V., Navarro, J.A., 2011. Contribution of topology determinants of a viral movement protein to its membrane association, intracellular traffic, and viral cell-to-cell movement. J. Virol. 85, 7797–7809. http://dx.doi.org/10.1128/JVI.02465-10.

Gowda, S., Satyanarayana, T., Robertson, C.J., Garnsey, S.M., Dawson, W.O., 2005. Infection of citrus plants with virions generated in *Nicotiana benthamiana* plants agroinfiltrated with a binary vector based *Citrus tristeza* virus. In: Proceedings of the 16th IOCV Conference, pp. 23–32.

Grangeon, R., Agbeci, M., Chen, J., Grondin, G., Zheng, H., Laliberté, J.-F., 2012. Impact on the endoplasmic reticulum and Golgi apparatus of turnip mosaic virus infection. J. Virol. 86, 9255–9265. http://dx.doi.org/10.1128/JVI.01146-12.

Han, S., Sanfaçon, H., 2003. Tomato ringspot virus proteins containing the nucleoside triphosphate binding domain are transmembrane proteins that associate with the endoplasmic reticulum and cofractionate with replication complexes. J. Virol. 77, 523–534. http://dx.doi.org/10.1128/JVI.77.1.523-534.2003.

Harries, P.A., Schoelz, J.E., Nelson, R.S., 2010. Intracellular transport of viruses and their components: utilizing the cytoskeleton and membrane highways. Mol. Plant–Microbe Interact. 23, 1381–1393. http://dx.doi.org/10.1094/MPMI-05-10-0121.

He, Y., Yang, Z., Hong, N., Wang, G., Ning, G., Xu, W., 2014. Deep sequencing reveals a novel closterovirus associated with wild rose leaf rosette disease. Mol. Plant Pathol. , http://dx.doi.org/10.1111/mpp.12202.

Heinlein, M., Padgett, H.S., Gens, J.S., Pickard, B.G., Casper, S.J., Epel, B.L., Beachy, R.N., 1998. Changing patterns of localization of the tobacco mosaic virus movement protein and replicase to the endoplasmic reticulum and microtubules during infection. Plant Cell 10, 1107–1120. http://dx.doi.org/10.1105/tpc.10.7.1107.

Hessa, T., Kim, H., Bihlmaier, K., Lundin, C., Boekel, J., Andersson, H., Nilsson, I., White, S.H., von Heijne, G., 2005. Recognition of transmembrane helices by the endoplasmic reticulum translocon. Nature 433, 377–381. http://dx.doi.org/10.1038/nature03216.

Hilf, M.E., Karasev, A.V., Pappu, H.R., Gumpf, D.J., Niblett, C.L., Garnsey, S.M., 1995. Characterization of *Citrus tristeza* virus subgenomic RNAs in infected tissue. Virology 208, 576–582. http://dx.doi.org/10.1006/viro.1995.1188.

Hofmann, K., Stoffel, W., 1993. TMbase—a database of membrane spanning proteins segments. Biol. Chem. HoppeSeyler 374, 166.

Huang, M., Zhang, L., 1999. Association of the movement protein of alfalfa mosaic virus with the endoplasmic reticulum and its trafficking in epidermal cells of onion bulb scales. Mol. Plant–Microbe Interact. , http://dx.doi.org/10.1094/MPMI.1999.12.8.680.

Ju, H.-J., Samuels, T.D., Wang, Y.-S., Blancaflor, E., Payton, M., Mitra, R., Krishnamurthy, K., Nelson, R.S., Verchot-Lubicz, J., 2005. The potato virus X TGBp2 movement protein associates with endoplasmic reticulum-derived vesicles during virus infection. Plant Physiol. 138, 1877–1895. http://dx.doi.org/10.1104/pp.105.066019.

Kaido, M., Funatsu, N., Tsuno, Y., Mise, K., Okuno, T., 2011. Viral cell-to-cell movement requires formation of cortical punctate structures containing red clover necrotic mosaic virus movement protein. Virology 413, 205–215. http://dx.doi.org/10.1016/j.virol.2011.02.008.

Karasev, A.V., 2000. Genetic diversity and evolution of closteroviruses. Phytopathology 90, 293–324.

Karasev, A.V., Boyko, V.P., Gowda, S., Nikolaeva, O.V., Hilf, M.E., Koonin, E.V., Niblett, C.L., Cline, K., Gumpf, D.J., Lee, R.F., Garnsey, S.M., Lewandowski, D.J., Dawson, W.O., 1995. Complete sequence of the *Citrus tristeza* virus RNA genome. Virology 208, 511–520. http://dx.doi.org/10.1006/viro.1995.1182.

Karasev, A.V., Hilf, M.E., Garnsey, S.M., Dawson, W.O., 1997. Transcriptional strategy of closteroviruses: mapping the 5′ termini of the citrus tristeza virus subgenomic RNAs. J. Virol. 71, 6233–6236.

Krishnamurthy, K., Heppler, M., Mitra, R., Blancaflor, E., Payton, M., Nelson, R.S., Verchot-Lubicz, J., 2003. The potato virus X TGBp3 protein associates with the ER network for virus cell-to-cell movement. Virology 309, 135–151. http://dx.doi.org/10.1016/S0042-6822(02)00102-2.

Laliberté, J.-F., Zheng, H., 2014. Viral manipulation of plant host membranes. Annu. Rev. Virol. 1, 237–259. http://dx.doi.org/10.1146/annurev-virology-031413-085532.

Laporte, C., Vetter, G., Loudes, A.-M., Robinson, D.G., Hillmer, S., Stussi-Garaud, C., Ritzenthaler, C., 2003. Involvement of the secretory pathway and the cytoskeleton in intracellular targeting and tubule assembly of Grapevine fanleaf virus movement protein in tobacco BY-2 cells. Plant Cell 15, 2058–2075. http://dx.doi.org/10.1105/tpc.013896.

Liu, J.-Z., Blancaflor, E.B., Nelson, R.S., 2005. The tobacco mosaic virus 126-kilodalton protein, a constituent of the virus replication complex, alone or within the complex aligns with and traffics along microfilaments. Plant Physiol. 138, 1853–1865. http://dx.doi.org/10.1104/pp.105.065722.

Lu, R., Folimonov, A., Shintaku, M., Li, W.-X., Falk, B.W., Dawson, W.O., Ding, S.-W., 2004. Three distinct suppressors of RNA silencing encoded by a 20-kb viral RNA genome. Proc. Natl. Acad. Sci. USA 101, 15742–15747. http://dx.doi.org/10.1073/pnas.0404940101.

Martínez-Gil, L., Johnson, A.E., Mingarro, I., 2010. Membrane insertion and biogenesis of the Turnip crinkle virus p9 movement protein. J. Virol. 84, 5520–5527. http://dx.doi.org/10.1128/JVI.00125-10.

Mathias, R.a., Chen, Y.-S., Kapp, E.a., Greening, D.W., Mathivanan, S., Simpson, R.J., 2011. Triton X-114 phase separation in the isolation and purification of mouse

liver microsomal membrane proteins. Methods 54, 396–406. http://dx.doi.org/10.1016/j.ymeth.2011.01.006.
McCartney, A.W., Greenwood, J.S., Fabian, M.R., White, K.A., Mullen, R.T., 2005. Localization of the tomato bushy stunt virus replication protein p33 reveals a peroxisome-to-endoplasmic reticulum sorting pathway. Plant Cell 17, 3513–3531. http://dx.doi.org/10.1105/tpc.105.036350.
McKeel, D.W., Jarett, L., 1970. Preparation and characterization of a plasma membrane fraction from isolated fat cells. J. Cell Biol. 44, 417–432.
Medina, V., Peremyslov, V.V., Hagiwara, Y., Dolja, V. V, 1999. Subcellular localization of the HSP70-homolog encoded by beet yellows closterovirus. Virology 260, 173–181. http://dx.doi.org/10.1006/viro.1999.9807.
Mitra, R., Krishnamurthy, K., Blancaflor, E., Payton, M., Nelson, R.S., Verchot-Lubicz, J., 2003. The potato virus X TGBp2 protein association with the endoplasmic reticulum plays a role in but is not sufficient for viral cell-to-cell movement. Virology 312, 35–48. http://dx.doi.org/10.1016/S0042-6822(03)00180-6.
Moreno, P., Ambrós, S., Albiach-Martí, M.R., Guerri, J., Peña, L., 2008. Citrus tristeza virus: a pathogen that changed the course of the citrus industry. Mol. Plant Pathol. , http://dx.doi.org/10.1111/j.1364-3703.2007.00455.x.
Nicholas, K.B., Nicholas, H.B.J., Deerfield, D.W.I., 1997. GeneDoc: analysis and visualization of genetic variation. EMBNEWS, p. 4.
Pappu, H.R., Karasev, A.V., Anderson, E.J., Pappu, S.S., Hilf, M.E., Febres, V.J., Eckloff, R.M., McCaffery, M., Boyko, V., Gowda, S., 1994. Nucleotide sequence and organization of eight 3′ open reading frames of the *Citrus tristeza* closterovirus genome. Virology 199, 35–46. http://dx.doi.org/10.1006/viro.1994.1095.
Peremyslov, V.V., Pan, Y., Dolja, V.V., 2004. Movement protein of a closterovirus is a type III integral transmembrane protein localized to the endoplasmic reticulum. J. Virol. 78, 3704–3709. http://dx.doi.org/10.1128/JVI.78.7.3704-3709.2004.
Reichel, C., Beachy, R.N., 1998. Tobacco mosaic virus infection induces severe morphological changes of the endoplasmic reticulum. Proc. Natl. Acad. Sci. USA 95, 11169–11174.
Restrepo-Hartwig, M., Ahlquist, P., 1999. Brome mosaic virus RNA replication proteins 1a and 2a colocalize and 1a independently localizes on the yeast endoplasmic reticulum. J. Virol. 73, 10303–10309.
Ritzenthaler, C., Laporte, C., Gaire, F., Dunoyer, P., Schmitt, C., Duval, S., Piéquet, A., Loudes, A.M., Rohfritsch, O., Stussi-Garaud, C., Pfeiffer, P., 2002. Grapevine fanleaf virus replication occurs on endoplasmic reticulum-derived membranes. J. Virol. 76, 8808–8819. http://dx.doi.org/10.1128/JVI.76.17.8808-8819.2002.
Robertson, C.J., Garnsey, S.M., Satyanarayana, T., Folimonova, S.Y., Dawson, W.O., 2005. Efficient infection of citrus plants with different cloned constructs of *Citrus tristeza* virus amplified in *Nicotiana benthamiana* protoplasts. In: Proceedings of the 16th IOCV Conference, pp. 187–195.
Satyanarayana, T., Bar-Joseph, M., Mawassi, M., Albiach-Martí, M.R., Ayllón, M.A., Gowda, S., Hilf, M.E., Moreno, P., Garnsey, S.M., Dawson, W.O., 2001. Amplification of Citrus tristeza virus from a cDNA clone and infection of citrus trees. Virology 280, 87–96. http://dx.doi.org/10.1006/viro.2000.0759.
Satyanarayana, T., Gowda, S., Ayllón, M.A., Dawson, W.O., 2004. Closterovirus bipolar virion: evidence for initiation of assembly by minor coat protein and its restriction to the genomic RNA 5′ region. Proc. Natl. Acad. Sci. USA 101, 799–804. http://dx.doi.org/10.1073/pnas.0307747100.
Satyanarayana, T., Gowda, S., Boyko, V.P., Albiach-Marti, M.R., Mawassi, M., Navas-Castillo, J., Karasev, A.V., Dolja, V., Hilf, M.E., Lewandowski, D.J., Moreno, P., Bar-Joseph, M., Garnsey, S.M., Dawson, W.O., 1999. An engineered closterovirus RNA replicon and analysis of heterologous terminal sequences for replication. Proc. Natl. Acad. Sci. USA 96, 7433–7438.
Satyanarayana, T., Gowda, S., Mawassi, M., Albiach-Martí, M.R., Ayllón, M.A., Robertson, C., Garnsey, S.M., Dawson, W.O., 2000. Closterovirus encoded HSP70 homolog and p61 in addition to both coat proteins function in efficient virion assembly. Virology 278, 253–265. http://dx.doi.org/10.1006/viro.2000.0638.
Schaad, M.C., Jensen, P.E., Carrington, J.C., 1997. Formation of plant RNA virus replication complexes on membranes: role of an endoplasmic reticulum-targeted viral protein. EMBO J. 16, 4049–4059. http://dx.doi.org/10.1093/emboj/16.13.4049.
Tatineni, S., Gowda, S., Dawson, W.O., 2010. Heterologous minor coat proteins of Citrus tristeza virus strains affect encapsidation, but the coexpression of HSP70h and p61 restores encapsidation to wild-type levels. Virology 402, 262–270. http://dx.doi.org/10.1016/j.virol.2010.03.042.
Tatineni, S., Robertson, C.J., Garnsey, S.M., Bar-Joseph, M., Gowda, S., Dawson, W.O., 2008. Three genes of *Citrus tristeza* virus are dispensable for infection and movement throughout some varieties of citrus trees. Virology 376, 297–307. http://dx.doi.org/10.1016/j.virol.2007.12.038.
Tatineni, S., Robertson, C.J., Garnsey, S.M., Dawson, W.O., 2011. A plant virus evolved by acquiring multiple nonconserved genes to extend its host range. Proc. Natl. Acad. Sci. USA , http://dx.doi.org/10.1073/pnas.1113227108.
Thomas, C.L., Bayer, E.M., Ritzenthaler, C., Fernandez-Calvino, L., Maule, A.J., 2008. Specific targeting of a plasmodesmal protein affecting cell-to-cell communication. PLoS Biol. 6, e7. http://dx.doi.org/10.1371/journal.pbio.0060007.
Thompson, J.D., Gibson, T.J., Plewniak, F., Jeanmougin, F., Higgins, D.G., 1997. The CLUSTAL_X windows interface: flexible strategies for multiple sequence alignment aided by quality analysis tools. Nucleic Acids Res. 25, 4876–4882.
Turner, K.A., Sit, T.L., Callaway, A.S., Allen, N.S., Lommel, S.A., 2004. Red clover necrotic mosaic virus replication proteins accumulate at the endoplasmic reticulum. Virology 320, 276–290. http://dx.doi.org/10.1016/j.virol.2003.12.006.
Tzanetakis, I.E., Martin, R.R., 2007. Strawberry chlorotic fleck: identification and characterization of a novel Closterovirus associated with the disease. Virus Res. 124, 88–94. http://dx.doi.org/10.1016/j.virusres.2006.10.005.
Ulmschneider, M.B., Sansom, M.S.P., 2001. Amino acid distributions in integral membrane protein structures. Biochim. Biophys. Acta—Biomembr. 1512, 1–14. http://dx.doi.org/10.1016/S0005-2736(01)00299-1.
van Der Heijden, M.W., Carette, J.E., Reinhoud, P.J., Haegi, A., Bol, J.F., 2001. Alfalfa mosaic virus replicase proteins P1 and P2 interact and colocalize at the vacuolar membrane. J. Virol. 75, 1879–1887. http://dx.doi.org/10.1128/JVI.75.4.1879-1887.2001.
von Heijne, G., 1991. Proline kinks in transmembrane alpha-helices. J. Mol. Biol. 218, 499–503. http://dx.doi.org/10.1016/0022-2836(91)90695-3.
Wang, J., Stewart, L.R., Kiss, Z., Falk, B.W., 2010. Lettuce infectious yellows virus (LIYV) RNA 1-encoded P34 is an RNA-binding protein and exhibits perinuclear localization. Virology 403, 67–77. http://dx.doi.org/10.1016/j.virol.2010.04.006.
Wimley, W.C., White, S.H., 1996. Experimentally determined hydrophobicity scale for proteins at membrane interfaces. Nat. Struct. Biol 3, 842–848. http://dx.doi.org/10.1038/nsb1096-842.
Woolhead, C.A., McCormick, P.J., Johnson, A.E., 2004. Nascent membrane and secretory proteins differ in FRET-detected folding far inside the ribosome and in their exposure to ribosomal proteins. Cell 116, 725–736. http://dx.doi.org/10.1016/S0092-8674(04)00169-2.
Yeh, H.H., Tian, T., Rubio, L., Crawford, B., Falk, B.W., 2000. Asynchronous accumulation of lettuce infectious yellows virus RNAs 1 and 2 and identification of an RNA 1 trans enhancer of RNA 2 accumulation. J. Virol. 74, 5762–5768. http://dx.doi.org/10.1128/JVI.74.13.5762-5768.2000.